107. Poly{[μ-(2,5-dicarboxypyrazine-3,6-dicarboxylato)-*trans*-diaquairon(II) dihydrate]}, a Member of a New Class of Quasi-Linear Chain Compounds. Preparation, Structure, and Magnetic Susceptibility

by **Pierre-Alain Marioni, Helen Stoeckli-Evans**, and **Werner Marty***

Institut de chimie, Université de Neuchâtel, Av. de Bellevaux 51, CH-2000 Neuchâtel

and **Hans-Ulrich Güdel**

Institut für anorganische und physikalische Chemie, Universität Bern, Freiestr. 3, CH-3000 Bern 9

and **Alan F. Williams**

Département de chimie minérale et analytique, Sciences II, Quai Ernest Ansermet 30, CH-1211 Genève 4

(23.IV.86)

The title compound **1**, $\{[Fe(H_2pztc)(H_2O)_2]\cdot 2\ H_2O\}_\infty$, has been prepared from pyrazinetetracarboxylic acid (H_4pztc) and Fe(II) salt in H_2O. It crystallizes in the monoclinic space group $P2_1/a$ with cell parameters $a = 13.56(1)$ Å, $b = 7.17(1)$ Å, $c = 6.48(1)$ Å, $\beta = 101.0(2)°$, $V = 618.4$ Å^3. The molecules form infinite parallel chains with bis(bidentate) coordination (through N and O) of the bridging pyrazine ligands. Two *trans*-COOH groups of the ligand remain uncoordinated, and two *trans*-H_2O ligands complete a pseudo-octahedral Fe(II) coordination which is distorted by the steric effect of the free COOH groups. The parallel polynuclear chains are linked through an extended network of H-bonds involving the COO functions of the bridging ligand and the coordinated and lattice H_2O molecules. *Mössbauer* and magnetic-susceptibility data suggest normal paramagnetic behaviour of high-spin Fe^{2+}. An observed drop below 15 K in effective magnetic moment for **1** was attributed to temperature-dependent population changes of the levels of the ground state $^5\Gamma$, and not to antiferromagnetic coupling ($J < 1$ cm^{-1}). This result establishes that the obvious potential magnetic exchange pathway through the pyrazine bridges is inefficient, and this may be attributed, in part, to the high planarity of Fe(H_2pztc) moieties.

Introduction. – Pyrazinetetracarboxylic acid (=H_4pztc) and its Na, K, and Ba salts as well as its Ag(I) complex have been known since 1893, [1] [2] but the potential of this easily accessible, bis(tridentate) binucleating ligand for the formation of quasi-linear coordination polymers has never been systematically investigated. This is surprising in view of the intense research activity presently directed at the synthesis and characterization of infinite coordination polymers [3]. In this report, we present one case of a *quasi-linear chain* compound, *viz.* **1**, $\{[Fe(H_2pztc)(H_2O)_2]\cdot 2\ H_2O\}_\infty$ obtained in a systematic study of the coordination chemistry of pyrazinetetracarboxylic acid with transition-metal ions.

Results and Discussion. – *Synthesis, Thermal Analysis, and Spectroscopic Characterization of* **1**. We have obtained a number of compounds of composition $M(I)_2[M'(II)(pztc)]\cdot n\ H_2O$ (M(I) = alkali metal, M'(II) = first-row transition metal, n = 0–6), [4] by reacting aqueous solutions of $M'(II)Cl_2$ or $M'(II)SO_4$ with 1 or more equiv. of H_4pztc, followed by the addition of $M(I)_2CO_3$ and EtOH. The same species were usually obtained irrespective of a wide variation of the M'(II)/H_4pztc ratio.

However, when no metal carbonate and EtOH were added in an otherwise identical procedure, the reaction mixture deposited crystals of the overall composition $M'(II)(H_2pztc)\cdot 4\,H_2O$ ($M'(II)$ = Fe, Co, Zn). These compounds were again obtained for a wide range of $M'(II)/H_4pztc$ ratios. Powder X-ray diffraction has shown these three compounds to be isomorphous, and comparison of the space group and cell parameters for the Fe and Zn compounds confirmed this.

Dark violet $[Fe^{II}(H_2pztc)(H_2O)_2]\cdot 2\,H_2O$, (**1**), was investigated in more detail. It was obtained under N_2, since in the presence of air, some Fe(III) was formed. Thermal gravimetry (TG) and differential thermal gravimetry (DTG) showed that the four H_2O molecules were lost pairwise with well-resolved DTG peaks at 120° and 165°. The dehydrated samples underwent decarboxylation ($-4\,CO_2$) in two separate, but overlapping steps with DTG peaks at 270° and 310°.

The *Mössbauer* spectrum of solid **1** at room temperature showed a single Fe site (isomer shift $(1.10 \pm 0.03)\ mm\cdot s^{-1}$, quadrupole splitting $(1.92 \pm 0.03)\ mm\cdot s^{-1}$, half width $(0.27 \pm 0.03)\ mm\cdot s^{-1}$). These data suggest high-spin Fe^{2+} in a pseudo-octahedral environment.

The IR spectrum shows intense bands at 3490 (br., with sh at *ca.* 3440 and 3990 cm^{-1}), 1950 (v. br.), 1710 (br.), and 1640 cm^{-1}. The last two overlapping absorptions are consistent with ν(C=O) in protonated and coordinated carboxylate groups, respectively. The group of absorptions near 3490 cm^{-1} is due in part to H_2O (coordinated and lattice H_2O, see below) as well as to free COOH. The δ(H–O–H) water absorption near 1630 cm^{-1} is obscured by the much stronger ν(C=O) bands. The 1950 cm^{-1} band arises from COOH H-bonding to H_2O, as it disappears upon dehydration at 120° of the sample. From the *Nakamoto-Rundle* empirical correlation [5], an O–H···O distance of (2.48 ± 0.04) Å is estimated for this H-bond. This estimate agrees well with the experimental value of 2.53(1) Å *(cf. Table 3)*.

X-Ray Structure Determination. Single-crystal X-ray diffraction *(Tables 1–3, Figs.1* and *2)* established that **1** is an infinite chain compound of Fe(II) with 2,5-dicarboxypyrazine-3,6-dicarboxylate (H_2pztc^{2-}) as the bridging ligand. The two COOH substituents do not coordinate, and H_2pztc^{2-} acts as a bis(bidentate) bridging ligand. Two *trans*-H_2O ligands complete a pseudo-octahedral coordination of each Fe center. The molecule has crystallographic C_i (= $\bar{1}$) symmetry. The pyrazine ring is planar to within 0.004(8) Å.

Distances and angles within the coordinated H_2pztc^{2-} ligand are similar to those in $[Fe(pyrazinecarboxylate)_2(H_2O)_2]$ (**2**) [6] except for the C(3)–O(1) distance of 1.231(11) Å which is shorter than that in **2** [6] by 0.04 Å. However, the Fe coordination in **1** is significantly different from that in **2** [6]: the Fe–N bond is 0.10 Å longer in **1**, whereas the Fe–O bond to the bound carboxylate is 0.035 Å shorter. These bond length differences have the expected consequences on the angles within the chelate ring (Table 3 and Fig. 1 in [6]). These structural differences may be attributed to the steric influence of the non-coordinated COOH groups, which are nearly perpendicularly oriented with respect to the plane of the pyrazine ring. The nonbonded O(1)···O(3) and O(1)···O(4) distances of 2.94 and 3.08 Å would become unreasonably short if the Fe–N bond in **1** was reduced to the value found in **2** [6]. This steric effect would also account for the 0.06 Å displacements of the pyrazine N-atoms on either side of the Fe–Fe axis.

From the observed O···O distances, all O-atoms except the Fe-bound carboxylate O-atom O(1) are involved in H-bonding. Thus, lattice H_2O molecules are linked to free

Table 1. *Crystal Data for* $\{[Fe(H_2pztc)(H_2O)_2]\cdot 2\,H_2O\}_\infty$[a])

Formula	$C_8H_{10}FeN_2O_{12}$
Formula wt.	382.03
Space group	monoclinic, $P2_1/a$
a [Å]	13.56(1)
b [Å]	7.17(1)
c [Å]	6.48(1)
β [°]	101.0(2)
V [Å^3]	618.4
Z	2
$d_{obs.}$ [gcm^{-3}]	1.99(2), by the flotation method in CH_3I/CCl_4
$d_{calc.}$ [gcm^{-3}]	2.051
Crystal dimensions [mm]	0.4 × 0.3 × 0.1
Radiation	Mo$K\alpha$, λ = 0.7107 Å (graphite monochromated)
Data collection	variable ω-scan technique [14] for layers h = 0–2, k = 0–6. $\Delta\omega = 1.0 + 0.5\,(\sin\mu/\tan\theta)$
θ limits	$5° \leqslant \theta \leqslant 26°$
No. of unique reflections	1376
No. of reflections used	718 ($I > 2.0\,\sigma(I)$)[b])
Absorption coefficient (μ_λ), cm^{-1}	12.1
Refinement method	full-matrix least squares
No. of reflections/No. of parameters	6.8
Final R value	0.069
Weighted final R value	$\Sigma w(\|F_o\| - \|F_c\|)/\Sigma wF_o = 0.077$
w	$[\sigma^2\|F_o\| + 0.00611\|F_o\|^2]^{-1}$ [12]
Parameter shift/e.s.d. in last cycle of refinement	0.08 (max); $\leqslant$ 0.04 (av.)

[a]) Standard deviation of the last significant figure in parentheses.
[b]) 4 reflections (probably suffering from extinction) removed.

Table 2. *Final Positional and Equivalent Isotropic Thermal Parameters*[a]) *for Non-H-Atoms in* $\{[Fe(H_2pztc)(H_2O)_2]\cdot 2\,H_2O\}_\infty$

Atom	x/a	y/b	z/c	U_{eq} [Å^2][b])
Fe	0.0	0.0	1.0	0.193(4)
N(1)	–0.0044(5)	0.3088(10)	1.0190(9)	0.0216(17)
C(1)	0.0529(6)	0.3885(13)	0.8952(12)	0.0211(22)
C(2)	0.0560(6)	0.5772(11)	0.8758(11)	0.0179(20)
C(3)	0.1129(6)	0.2551(14)	0.7823(12)	0.0201(20)
C(4)	0.1169(7)	0.6806(12)	0.7388(12)	0.0250(22)
O(1)	0.0956(5)	0.0887(8)	0.8050(9)	0.0238(16)
O(2)	0.1761(4)	0.3224(9)	0.6879(9)	0.0271(16)
O(3)	0.0828(5)	0.7195(9)	0.5586(8)	0.0298(16)
O(4)	0.2049(5)	0.7332(9)	0.8488(9)	0.0316(17)
O(W1)	–0.1219(4)	0.0179(8)	0.7386(9)	0.0295(15)
O(W2)	0.2010(5)	0.4866(9)	0.3055(9)	0.0332(17)
H1(W1)	–0.1744	0.0030	0.7693	
H1(W2)	0.1759	0.4276	0.4430	
H(04)	0.2446	0.7972	0.7471	

[a]) E.s.d.'s in parentheses.
[b]) $U_{eq} = \frac{1}{3}\sum_i\sum_j U_{ij}a^*_i a^*_j \vec{a}_i\cdot\vec{a}_j$.

Table 3. *Bond Distances* [Å] *and Angles* [°][a])

Fe–N(1)	2.219(8)	C(4)–O(3)	1.203(10)
Fe–O(1)	2.075(6)	C(4)–O(4)	1.323(10)
Fe–O(W1)	2.133(6)	O(W1)–H1(W1)	0.782
N(1)–C(1)	1.346(10)	O(W2)–H1(W2)	1.098
N(1)–C(2^{i})	1.344(11)	O(W2)···O(2)	2.82(1)
C(1)–C(2)	1.360(14)	H1(W2)···O(2)	1.757
C(1)–C(3)	1.530(13)	O(4)–H(O4)	1.035
C(2)–C(4)	1.516(12)	O(4)···O(W2^{ii})	2.53(1)
C(3)–O(1)	1.231(11)	H(O4)···O(W2^{ii})	1.613
C(3)–O(2)	1.242(10)	O(3)···O(W1^{iii})	2.82(1)
		O(1^{iv})···O(3)	3.08(1)
		O(1^{iv})···O(4)	2.94(1)
		O(2)···O(3)	3.16(1)
		O(2)···O(4)	3.12(1)
O(W1)–Fe–N(1)	87.7(2)	C(1)–C(2)–C(4)	124.8(8)
O(W1)–Fe–O(1)	88.7(2)	N(1^{i})–C(2)–C(4)	113.2(8)
O(1)–Fe–N(1)	75.8(2)	C(1)–C(3)–O(1)	114.7(7)
Fe–N(1)–C(1)	111.5(6)	C(1)–C(3)–O(2)	118.3(9)
Fe–N(1)–C(2^{i})	131.1(7)	O(1)–C(3)–O(2)	127.0(9)
C(1)–N(1)–C(2^{i})	117.4(6)	C(2)–C(4)–O(3)	122.1(8)
Fe–O(1)–C(3)	121.7(5)	C(2)–C(4)–O(4)	111.1(7)
N(1)–C(1)–C(2)	120.7(8)	O(3)–C(4)–O(4)	126.6(8)
N(1)–C(1)–C(3)	116.1(8)	O(W2)–H1(W2)···O(2)	162
C(2)–C(1)–C(3)	123.2(8)	O(4)–H(O4)···O(W2^{ii})	145
C(1)–C(2)–N(1^{i})	122.0(8)		

[a]) Symmetry operations: i $-x, 1-y, 2-z$; ii $\frac{1}{2}-x, \frac{1}{2}+y, 1-z$; iii $-x, 1-y, 1-z$; iv $x, 1+y, z$.

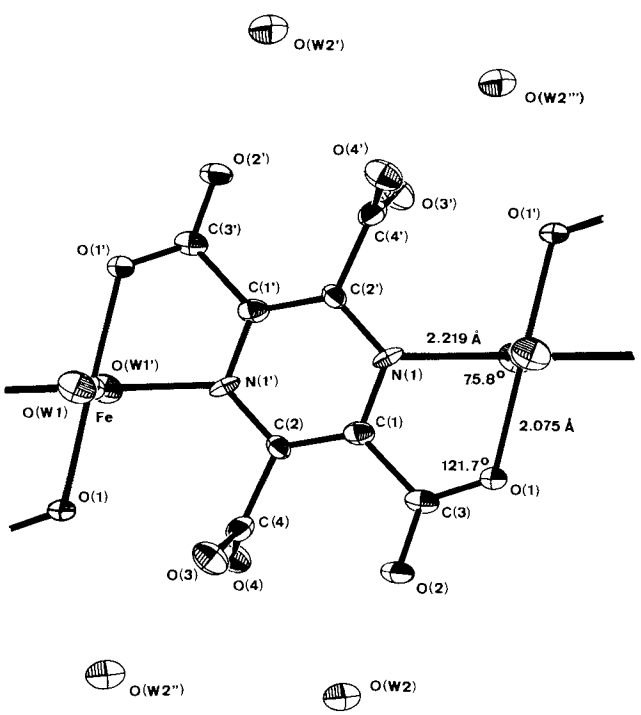

Fig. 1. *ORTEP* [15] *drawing of the molecule showing the atom-numbering scheme and the vibrational ellipsoids* (50% probability level). A center of symmetry relates atom O(W2) to O(W2'), two-fold screw axes relate atom O(W2) to O(W2''), and O(W2') to O(W2''').

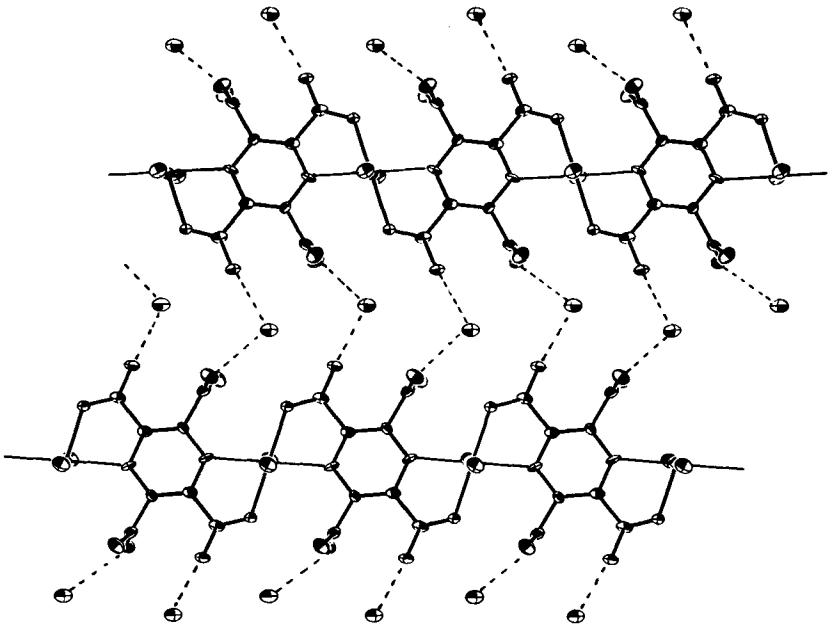

Fig. 2. *Perpendicular view of two parallel* $\{[Fe(H_2pztc)(H_2O)_2]\cdot 2\ H_2O\}_\infty$ *chains, showing the 'in-plane' H-bonds that lead to the formation of sheets of the above chains.* The impression of the merging of the chains created by this drawing is an optical illusion, similar to the well-known, simple diagram:

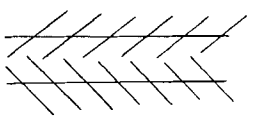

COOH O-atoms O(4) as well as to the carbonyl O-atoms O(2) of the coordinating carboxylate of a symmetry-related chain. In this way, the $Fe(H_2pztc)(H_2O)_2$ chains form sheets that are inclined by 39.9° with respect to the *ab* plane. These sheets are stacked in the *c* direction and separated by a perpendicular distance of 5 Å. The sheets are linked through H-bonding between the coordinated H_2O molecules O(W1) and the carbonyl O-atoms O(3) of the COOH function of a chain displaced by one unit cell in the *c* direction. In contrast, H-bonding in anhydrous **2** [6] involves interactions between the coordinated H_2O ligands and the two carboxylate O-atoms of two adjacent molecules.

Magnetic Behaviour. Magnetic susceptibility data on **1** were measured in the range 1.3–310 K by the moving-sample technique [7]. *Fig. 3* shows plots of the inverse magnetic susceptibility χ_A^{-1} *vs.* T in the range 4–310 K and the conventional effective magnetic moment μ_{eff} as a function of T (1.3–20 K) for **1**. The quantities χ_A and μ_{eff} are related by $\chi_A = (N\mu_B^2/3kT)\mu_{eff}^2$. Above 20 K, μ_{eff} was nearly constant. Between 4 and 300 K, the data show no significant deviation from the *Curie* law:

$$1/\chi_A = 3kT/Ng^2\mu_B^2S(S+1). \quad (1)$$

A least-squares fit of *Eqn. 1* gave $g = 2.11$ *(Fig. 3)*, in good agreement with g values of high-spin Fe(II) centers in similar environments [6] and consistent with nearly complete

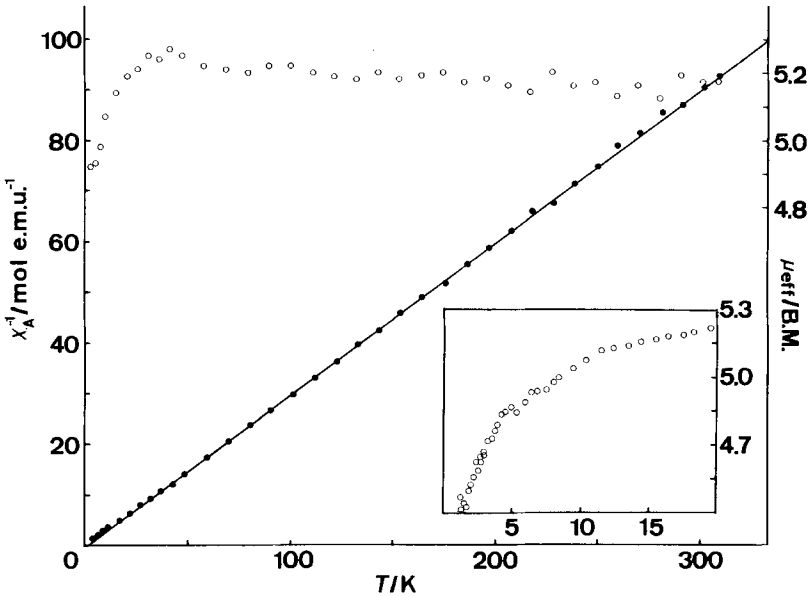

Fig. 3. *Inverse atomic susceptibility* χ_A^{-1} vs. T *for* $\{[Fe(H_2pztc)(H_2O)_2]\cdot 2\ H_2O\}_\infty$ (full circles). Line drawn using g = 2.11 from least-squares fit. Empty circles and inset: μ_{eff} *vs. T.*

quenching of the orbital angular momentum. This quenching was to be expected for structure **1** where the actual approximate point symmetry of the Fe^{2+} ions is C_{2v}, with substantial deviations from the idealized D_{4h} FeN_2O_4 coordination. The magnetic properties are, therefore, dominated by one-orbital singlet, spin quintet state $^5\Gamma$. For a rough estimate of parameters, we assume axial symmetry. The spin-orbit coupling parameter λ was set to the free-ion value of -100 cm^{-1} [8]. The axial crystal-field parameter Δ was varied between $+1000$ and -1000 cm^{-1}. Both perturbations (in the $^5T_2$ basis) were treated simultaneously. A reasonably accurate description of the observed temperature dependence of μ_{eff} was obtained for $\Delta = 1000$ cm^{-1}, *i.e.* the orbital singlet $^5\Gamma$ ground state is separated by 1000 cm^{-1} from the higher-energy components. For this combination of parameters, $^5\Gamma$ is split into the components $|M = 0>$, $|M = \pm 1>$ and $|M = \pm 2>$, separated by 11 and 34 cm^{-1}, respectively.

The observed drop of magnetic moment below 15 K may result from the splitting of $^5\Gamma$ [8], or alternatively, from antiferromagnetic exchange interactions, most likely within the chains of H_2pztc^{2-} bridged Fe(II) ions. Distinction between these two mechanisms was possible by measuring the susceptibility of a magnetically dilute crystalline powder of isostructural $\{[Zn(H_2pztc)(H_2O)_2]\cdot 2\ H_2O\}_\infty$ containing $(4.63 \pm 0.07)\%$ of Fe^{2+}. The magnetic behavior of this sample was consistent with that of undiluted **1** and thus suggests that antiferromagnetic chain interactions across the pyrazine bridges or across the H-bonds are negligible down to 1.3 K. Compound **1** shows normal paramagnetic behaviour between 1.3 and 310 K. In comparison, **2** shows antiferromagnetic interactions, mediated through a three-atom Fe–O–H···O–Fe pathway [6]. In **1**, an exchange pathway through the H-bonds would involve at least eight atoms. Thus, the most

likely pathway for exchange interactions is along the chains and through the conjugated π system of the bridging ligand. From the absence of detectable exchange effects in the magnetic data down to 1.3 K, we can estimate that the exchange parameter **J** must be smaller than 1 cm^{-1}. A possible reason for this very low value may lie in the high planarity of the bridging geometry, which essentially prevents all but two of the unpaired electrons per Fe^{2+} ion from contributing to the exchange. In addition, it should be borne in mind that **J** may be composed of antiferromagnetic and ferromagnetic orbital contributions, with the possibility of partial cancellation.

Conclusion. –The infinite linear chain compound **1** is significant in several respects. All chains in the structure are parallel which leads to maximal anisotropy of the lattice. In contrast, the infinite chains in the loosely related compound, bis(2,3-dicarboxylatopyrazine)copper(II) [9] are oriented along two different directions. The chains in compound **1** are nearly rectilinear, and within the chelated $Fe(H_2pztc)$ moieties the pyrazine rings cannot be tilted with respect to the principal plane of coordination of the Fe^{2+} centers. An untilted orientation of unsubstituted pyrazine ligand bridges has been found previously in $[Cu(hexafluoroacetylacetonate)_2(pyrazine)]_\infty$, and the coplanar arrangement of the pyrazine bridges with respect to one coordination plane of Cu^{2+} was held responsible for the lack of measurable magnetic interactions [10].

Finally, since **1** is formed irrespective of the metal/ligand ratio within wide limits (see above), it is worthy of note that compound **1** is formed and not a mixture of H_4pztc and $(H_2O)_3Fe(pztc)Fe(OH_2)_3$. This may possibly be explained by the lack of strain in bidentate $Fe(H_2pztc)$ moieties, relative to the strained situation of a tridentate Fe(pztc) fragment, where a shorter Fe–N bond and smaller O–Fe–N angles are expected.

Experimental. – $\{[Fe(H_2pztc)(H_2O)_2]\cdot 2\,H_2O\}_\infty$. A soln. of H_4pztc [11] (1.20 g, 4.69 mmol) in deoxygenated H_2O (30 ml) was heated to 40°. It was then added dropwise, with stirring and under N_2, to a filtered soln. of $FeCl_2\cdot 4\,H_2O$ (*Fluka, puriss.*; 0.90 g, 4.53 mmol) in deoxygenated H_2O (15 ml). The intense blue-violet mixture was stirred for 10 min at 40° and evaporated (*Rotavap*) to 35 ml. Further evaporation leads to precipitation of the free ligand. The soln. was then left under N_2 and in the dark for 5 d at r.t. Filtration affords dark-blue-violet crystals with olive brown dichroism, which are readily soluble in H_2O. Yield 0.72 g (42%). Anal. calc. for $C_8H_{10}FeN_2O_{12}$: C 25.15, H 2.64, N 7.33, Fe 14.62; found: C 25.23, H 2.81, N 7.33, Fe 14.85.

Spectroscopic Measurements. Mössbauer spectra were measured with a conventional constant acceleration spectrometer. Isomer shifts are relative to Fe metal. IR spectra on CsBr pellets were recorded on a *Perkin-Elmer IR 521* instrument.

Crystal-Structure Determination. Preliminary *Weissenberg* and precession photographs served to determine the space group. Intensity data were measured on a *Stoe STADI-2* two-circle diffractometer at r.t. Accurate cell dimensions were obtained by the centering of axial reflections. The SHELX-76 program system [12] was used for solving the structure, by *Patterson* and *Fourier* methods, and in further calculations. Scattering factors were taken from [12] [13].

In the final cycles of refinement, one H-atom of each H_2O molecule and that of O(4)–H were included in observed positions but not refined ($U_{iso} = 0.10$). It was not possible to locate the second H-atom of the H_2O molecules. The largest peak in the final difference map was 0.90 $eÅ^{-3}$, at *ca.* 1 Å from the Fe-atom. Tables of final observed and calculated structure factors *etc.* are available from *H. St.-E.*

This work was supported by the *Swiss National Science Foundation* (project 2.838–0.83). We thank *K. Mattenberger* for the susceptibility measurements.

REFERENCES

[1] L. Wolff, *Ber. Deutsch. Chem. Ges.* **1887,** *20,* 425.
[2] L. Wolff, *Ber. Deutsch. Chem. Ges.* **1893,** *26,* 721.
[3] W.E. Hatfield, W.E. Estes, W.E. Marsh, M.W. Pickens, L.W. ter Haar, R.R. Weller, in 'Extended Linear Chain Compounds', Ed. J.S. Miller, Plenum Press, New York, 1983, Vol. 3, pp. 43–133.
[4] P.-A. Marioni, unpublished results.
[5] K. Nakamoto, M. Margoshes, R.E. Rundle, *J. Am. Chem. Soc.* **1955,** *77,* 6480 *(Fig. 1)*.
[6] C.L. Klein, C.J. O'Connor, R.J. Majeste, L.M. Trefonas, *J. Chem. Soc., Dalton Trans.* **1982,** 2419.
[7] J.P. Rebouillat, Thèse de doctorat, CNRS, Grenoble, 1972.
[8] F.E. Mabbs, D.J. Machin, 'Magnetism and Transition Metal Complexes', Chapman and Hall, London, 1973, p. 128.
[9] C.J. O'Connor, C.L. Klein, R.J. Majeste, L.M. Trefonas, *Inorg. Chem.* **1982,** *21,* 64.
[10] H.W. Richardson, J.R. Wasson, W.E. Hatfield, *Inorg. Chem.* **1977,** *16,* 484.
[11] F.D. Chattaway, W.G. Humphrey, *J. Chem. Soc.* **1929,** 645.
[12] G.M. Sheldrick, 'SHELX-76' Program for Crystal Structure Determination. University of Cambridge, G.B.
[13] 'International Tables for X-Ray Crystallography', Kynoch Press, Birmingham, 1976, Vol. IV, pp. 99, 149.
[14] H.C. Freeman, J.M. Guss, C.E. Nuckolds, R. Page, A. Webster, *Acta Crystallogr., Sect. A* **1970,** *26,* 149.
[15] C.K. Johnson, 'ORTEP-II', Oak Ridge National Laboratory Report 5138, Oak Ridge National Laboratory, Oak Ridge, Tennessee, 1976.